

SEG TDR 64-16

67,485

**STRESS ANALYSIS OF THE EXTERNAL FRONT
WINDOW OF THE X-20A (DYNA-SOAR).**

✓
VERNER J. JOHNSON

TECHNICAL DOCUMENTARY REPORT No. SEG TDR 64-16

JUNE 1964
✓

X-20 ENGINEERING OFFICE
SYSTEMS ENGINEERING GROUP
RESEARCH AND TECHNOLOGY DIVISION
= US AIR FORCE SYSTEMS COMMAND.
WRIGHT-PATTERSON AIR FORCE BASE, OHIO

PROPERTY OF
LTV VOUGHT AERONAUTICS DIVISION
System 620A
LIBRARY

JUN 22 1965

NOTICES

When Government drawings, specifications, or other data are used for any purpose other than in connection with a definitely related Government procurement operation, the United States Government thereby incurs no responsibility nor any obligation whatsoever; and the fact that the Government may have formulated, furnished, or in any way supplied the said drawings, specifications, or other data, is not to be regarded by implication or otherwise as in any manner licensing the holder or any other person or corporation, or conveying any rights or permission to manufacture, use, or sell any patented invention that may in any way be related thereto.

Qualified requesters may obtain copies of this report from the Defense Documentation Center (DDC), (formerly ASTIA), Cameron Station, Bldg. 5, 5010 Duke Street, Alexandria, Virginia, 22314.

This report has been released to the Office of Technical Services, U.S. Department of Commerce, Washington 25, D. C., in stock quantities for sale to the general public.

Copies of this report should not be returned to the Research and Technology Division, Wright-Patterson Air Force Base, Ohio, unless return is required by security considerations, contractual obligations, or notice on a specific document.

400 - July 1964 - 162-45-938

SEG TDR 64-16

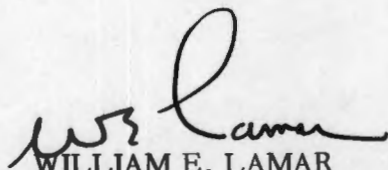
FOREWORD

This report was prepared by personnel of the X-20 Engineering Office. It is the stress analysis of the external front window of the X-20A. The author especially acknowledges the help of task engineers Laslow Berke and James Johnson of the Air Force Flight Dynamics Laboratory in the use of the computer program and for their aid in this study. X-20 Engineering Office Project Engineers, W. D. Cowie and Captain R. J. Meyette, supplied drawings of the window and the design pressure distribution for that window, respectively. Messrs. R. M. Bader and F. Campanile derived the temperature distribution.

ABSTRACT

The structure of the external front window of the X-20A is analyzed. A sophisticated matrix method of analysis, rather than a classical analytic method, was used to determine the behavior of a window of the X-20A re-entry vehicle under loads and temperatures. A computer solution provides results that can be used for future developments of re-entry vehicles and reveals areas that should be given further study.

This technical documentary report has been reviewed and is approved.



WILLIAM E. LAMAR
Director,
X-20 Engineering Office,
Systems Engineering Group

TABLE OF CONTENTS

	PAGE
INTRODUCTION	1
GEOMETRY AND MATERIALS	1
IDEALIZATION	2
DESIGN CONDITION	5
INTERPRETATION	5
RESULTS	7
EVALUATION	8
CONCLUSIONS	9
RECOMMENDATIONS	9
REFERENCES	10

LIST OF ILLUSTRATIONS

Figure		Page
1	X-20A Glide Re-entry Vehicle	11
2	Isometric View of Window	12
3	Section of Window Glass	13
4	Section of Window Frame	14
5	Seal Cross-Section	15
6	Isometric View of Structural Model	16
7	Working Drawing of Structural Model	17
8	Design Pressure Distribution	18
9	Design Temperature Distribution	19
10	Typical Load Distribution Due to Airloads	20
11	Typical Load Distribution Due to Temperature	21
12	Deflections Due to Airloads	22
13	Thermal Deflections	23
14	Total Deflections	24
15	Surface Tensile Stresses Due to Airloads	25
16	Surface Tensile Stresses Due to Temperature	26
17	Total Surface Tensile Stresses	27
18	Results of Approximate Stress Analysis	28
19	Fused Silica Glass Design Allowables	29

SYMBOLS

a	seal section length
b	seal section width
\bar{b}	panel width
c	distance from neutral axis to outer fibers
d	cross-section width
\bar{d}	panel thickness
f	stress
k	radius of gyration
p	pressure
t	thickness
A	cross-sectional area
E	modulus of elasticity
FS	factor of safety
I	moment of inertia
M	bending moment
P	internal load
T	uniform temperature
ΔT	linear temperature gradient
T^*	self-equilibrating temperature
\bar{z}	distance from neutral axis to average load
α	linear thermal expansion coefficient
ϵ	strain
ν	poisson's ratio

SUBSCRIPTS

1	outer surface
2	middle surface
3	inner surface
i	ideal
m	mean
\bar{A}	outer frame section
\bar{B}	inner frame section
C	cooler surface
H	hotter surface
N	neutral axis
R	real
av	average

SUPERSCRIPTS

*	self-equilibrating
---	--------------------

INTRODUCTION

Unmanned re-entry vehicles have no windows; it was the ballistic manned system that fostered a desire for observation windows although no vital need for them existed. In a controlled re-entry vehicle, the pilot will need windows during the re-entry, the approach, and the landing phases to successfully complete the mission. Exposure to the re-entry environment complicates window design because the materials used must resist re-entry airloads and temperatures. Unfortunately, heat-resistant window materials are inherently brittle and of low tensile strength. The window, therefore, must be designed to eliminate areas of high tensile stress, and the analysis of the window must be sophisticated to accurately reveal the behavior of the window under load and temperature.

Classical analytic methods cannot provide an accurate account of the behavior of the window. Such methods inadequately account for window and frame interaction, boundary conditions, and deflections. The deficiencies of the classical analytical methods are overcome by the more sophisticated matrix methods that are widely used in the aerospace industry. A general matrix force computer program, developed by the Douglas Aircraft Company, was used to study the windows of the X-20A glide re-entry vehicle.

GEOMETRY AND MATERIALS

Visibility in three directions will be provided by five pilot's compartment windows in the X-20A vehicle. Figure 1 illustrates the location of the window studied. It is the No. 1 window. The total cross-sectional configuration consists of two windows. The external window is part of the external structure, and the laminated internal window is part of the internal pressure can. This document reports an analysis of the internal No. 1 window.

The No. 1 window will be a symmetric trapezoid with rounded corners enclosed in a complex frame. The window thickness is uniform except for a border of reduced thickness on the outer face. The outer face will be flush with the adjacent glider structure when combined with the window seal and the frame. The detailed configuration is shown in Figure 2.

The window and frame materials are fused silica glass and Rene' 41, respectively. Fused silica is a low modulus glass, and Rene' 41 is a nickel-base alloy. Both materials have a long-time working temperature limit of 1800°F (Reference 1). Glass expansion at increased temperature in the plane of the glass is retarded only by contact with the seal and frame. The frame expansion is limited by the surrounding glider structure. This resistance to thermal growth induces load into the glass. Additional loads in the glass are caused by airloads which accompany the temperature. This combination of external loads causes axial and bending deformations in the window. The response must be reflected by the idealization of the structure.

Manuscript released by the author 31 March 1964 for publication as an RTD Technical Documentary Report.

IDEALIZATION

Information on the development of matrix formulae is available in standard references (References 2, 3, and 4). Pertinent formulae were programmed for digital computation by the Douglas Aircraft Company (Reference 5). The program may be applied to any structure provided a suitable idealization can be constructed from two types of elements.

The elements are beams that resist forces and moments and panels that resist shear. Both types of elements are not used in all cases, e.g., a truss may be represented by beams alone. Both types are used to represent a continuous structure. The simplest legitimate combination of both elements is a panel with beams at its four edges. The bars and panel edges are joined at their midpoints. Assemblies of this combination of elements constitute the idealized structure.

Relations between ideal and real structures depend upon the item to be analyzed. The responses of the window to its external loads are bending and axial deformations that produce axial and bending stresses. Area and moment of inertia are the pertinent geometric terms. The nonlinear temperature profile through the glass is approximated in the ideal window. Ideal elements are assigned temperatures, depending upon their levels, through the thickness. The number of nodes is limited by the digital computer core storage capacity. Three levels of elements in the ideal structure transfer the axial and bending loads. Figure 3 shows a section of the glass. Two definitions are made: (a) $A_1 = A_3$; and (b) $I_1 = I_3$. Element dimensions are derived by equating areas and moments of inertia of the ideal and real structures:

$$\begin{aligned}\sum A_i &= A_1 + A_2 + A_3 \\ &= 2A_1 + A_2\end{aligned}$$

$$A_R = dt$$

$$\sum A_i = A_R$$

$$2A_1 + A_2 = dt$$

$$\sum I_i = I_1 + I_2 + I_3$$

$$I_1 = I_3 = k_1^2 A_1$$

$$= \left(\frac{1}{2}\right)^2 A_1$$

$$I_2 = k_2^2 A_2$$

$$= (0) A_2$$

$$= 0$$

$$\sum I_i = 2 \left(\frac{1}{2}\right)^2 A_1 + 0$$

$$I_R = \frac{dt^3}{12}$$

$$\sum I_i = I_R$$

$$t^2 \frac{A_i}{2} = \frac{dt^3}{12}$$

$$\therefore A_1 = A_3 = \frac{dt}{6}$$

$$A_2 = \sum A_i - (A_1 + A_3)$$

$$= dt - \frac{dt}{3}$$

$$= \frac{2dt}{3}$$

Similar relations exist between the ideal and real structures for the window frame and for the seals, which are shown in detail in Figure 2. The window frame under load resists bending. It is affected by the temperature gradient as the glass is, and the same mathematical relations hold. For this component, two levels are assumed to approximate the temperature gradient. Figure 4 shows a section of the frame. Element dimensions and radii of gyration are derived as follows:

$$\sum A_i = A_{\bar{A}i} + A_{\bar{B}i}$$

$$A_R = A_{\bar{A}R} + A_{\bar{B}R}$$

$$\sum A_i = A_R$$

$$A_{\bar{A}i} + A_{\bar{B}i} = A_{\bar{A}R} + A_{\bar{B}R}$$

$$A_{\bar{A}i} = A_{\bar{A}R}, A_{\bar{B}i} = A_{\bar{B}R}$$

$$\sum I_i = I_{\bar{A}i} + I_{\bar{B}i}$$

$$= k_{\bar{A}i}^2 A_{\bar{A}i} + k_{\bar{B}i}^2 A_{\bar{B}i}$$

$$= k_{\bar{A}i}^2 A_{\bar{A}R} + k_{\bar{B}i}^2 A_{\bar{B}R}$$

$$I_R = I_{\bar{A}R} + I_{\bar{B}R}$$

$$\sum I_i = I_R$$

$$k_{\bar{A}i}^2 A_{\bar{A}R} + k_{\bar{B}i}^2 A_{\bar{B}R} = I_{\bar{A}R} + I_{\bar{B}R}$$

$$k_{\bar{A}i}^2 A_{\bar{A}R} = I_{\bar{A}R}, k_{\bar{B}i}^2 A_{\bar{B}R} = I_{\bar{B}R}$$

$$k_{\bar{A}i} = \left[\frac{I_{\bar{A}R}}{A_{\bar{A}R}} \right]^{\frac{1}{2}}, k_{\bar{B}i} = \left[\frac{I_{\bar{B}R}}{A_{\bar{B}R}} \right]^{\frac{1}{2}}$$

The significance here of radii of gyration is that they are the locations of the idealized frame elements in relation to the neutral axis. The seal, which is between the glass and the frame, is shown in Figure 2. Like the glass and the frame, relations for the seals exist between the real and the ideal structures. 3

The seal is supported between the frame and the glass. A leaf spring arrangement, which is part of the frame, holds the seal in place. Load is transferred between the frame and the glass through the seal by a distributed axial force. In the idealized structure, the distributed force is lumped into axial force members. They are joined to the glass and frame idealizations by pinned joints. The pinned joints simulate the slippage that occurs between the window and the frame in the real structure. Figure 5 shows a section of the window seal.

From a relation between the real and the model seals, the cross-sectional areas of the lumped force members were derived as follows:

$$\epsilon_R = \frac{PL_R}{A_R E} = \frac{PL_R}{\sigma_R b_R E}$$

$$\epsilon_i = \frac{PL_i}{A_i E}$$

$$\epsilon_R = \epsilon_i$$

$$\frac{PL_R}{\sigma_R b_R E} = \frac{PL_i}{A_i E}$$

$$\frac{L_R}{\sigma_R b_R} = \frac{L_i}{A_i}$$

$$L_i = k_i - \frac{t}{2}$$

where

k_i = radii of gyration for the frame members

$t/2$ = distance between neutral axis and glass surface.

Then

$$\frac{L_R}{\sigma_R b_R} = \frac{k_i - \frac{t}{2}}{A_i}$$

$$A_i = \frac{k_i - \frac{t}{2}}{L_R} \times \sigma_R b_R$$

These are the primary elements for the structural model of the No. 1 window. Because of longitudinal symmetry of the design and of the external loads, longitudinal symmetry of the model also was assumed. The completed structural model is shown in Figure 6. The working drawing of the model is shown in Figure 7.

DESIGN CONDITION

Briefly, an X-20A mission will consist of boost, orbit, re-entry, approach, and tangential landing. During the boost and orbital phases, the three forward-facing windows are protected by a heatshield that will be ejected during re-entry to allow forward visibility during approach and landing. The critical condition occurs immediately after the heatshield ejection. The net pressure distribution in Figure 8 was concentrated at the surface nodes of the model. The temperature distribution of Figure 9 was uniformly applied, except for edge effects, which increase the temperature gradient in the frame.

INTERPRETATION

Interpretation may be defined as the reverse of the idealization procedure. Idealization is the construction of a model based on the probable behavior of the structure. Interpretation is the study of structural behavior based on the idealization. If this cycle is followed without discrepancies arising, some measure of confidence is developed.

The interpretation was divided into airload and temperature effects. This division is not only convenient, but it is also desirable since a comparison of the separate and overall effects may show problem areas and areas for effective redesign.

Airloads applied to the window cause deflections normal to the glass plane. This deflection produces bending stresses that are linear across the section. Stresses are greatest at the surfaces and nil at the neutral axis. A typical distribution of load is shown in Figure 10. This distribution conforms to the definition of bending applied to the ideal structure. The derivation of stresses due to airloads relates the ideal and real structures:

$$M_i = P_{Av} \times \bar{z}$$

$$M = \sum M_i$$

$$C = \pm \frac{t}{2}$$

$$I = \frac{dt^3}{12}, \text{ derived during the idealization}$$

$$\sigma = \pm \frac{MC}{I} = \pm \frac{2PA}{dt}$$

Similar formulae may be developed for stresses that are due to the temperature gradient through the glass.

Thermal effects in the glass may be divided into three parts; effects of uniform, linear, and non-linear temperature gradients. These gradients produce uniform and non-linear axial, as well as, bending deformations and stresses. The corresponding loads are carried by the cross-sectional elements of the ideal structure shown in Figure 11. This is expressed by three simultaneous equations which represent the three elements through the section:

$$P_{AH} + P_{BH} + P_{CH} = P_H$$

$$P_{AN} + P_{BN} + P_{CN} = P_N$$

$$P_{AC} + P_{BC} + P_{CC} = P_C$$

where, by definition of axial and bending stresses,

$$(P_A)_{H,N,C} = -(\sigma_A) (A)_{H,N,C}$$

$$(P_B)_{H,C} = \pm(\sigma_B)_{H,C} \left[\frac{I}{(\bar{Z})_{H,C}} (C)_{H,C} \right]$$

$$(P_B)_N = 0$$

$$(P_C)_{H,C} = -(\sigma_C)_{H,C} (A)_{H,C}$$

$$(P_C)_N = + 0.5 (\sigma_C)_N (A)_N$$

$$A_H = A_C = \frac{A_N}{4}$$

From the idealization and from Figure 11 further simplification is possible by substituting as follows:

$$A_H = \frac{dt}{6}$$

$$C = \frac{t}{2}$$

$$\bar{z} = \frac{2}{3} C = \frac{t}{3}$$

$$I = \frac{dt^3}{12}$$

When we solve the simultaneous equations for σ_A , σ_B , and σ_C we obtain

$$\sigma_A = - \frac{P_H + P_N + P_C}{dt}$$

$$\sigma_B = \frac{P_H - P_C}{dt}$$

$$\sigma_C = \frac{-2P_H + P_N - 2P_C}{dt}$$

which allow easy tabular solutions.

Total thermal stress on each ideal element is then

$$\begin{aligned}\sigma_H &= -\sigma_A + \sigma_B - \sigma_C \\ &= \frac{4P_A + 2P_C}{dt}\end{aligned}$$

$$\begin{aligned}\sigma_N &= -\sigma_A + 0.5 \sigma_B \\ &= \frac{1.5 P_B}{dt}\end{aligned}$$

$$\sigma_C = \frac{2P_A + 4P_C}{dt}$$

Superposed stresses due to airloads and temperatures are

$$\sigma = \sigma_{\text{AIRLOAD}} + \sigma_{\text{TEMPERATURE}}$$

The failure theory that best applied to brittle materials is the maximum strain theory. It states that inelastic action begins when the maximum strain equals the strain where uniaxial stress causes inelastic action to begin. In brittle materials, the critical uniaxial stress is tensile. The associated strain is $\epsilon = \sigma/E$. The tensile stress and strain allowables for fused silica are shown in Figure 19.

In a body subjected to triaxial strain, the state of strain is

$$\epsilon = \left(\frac{\sigma_1}{E}\right) - \nu \left(\frac{\sigma_2}{E}\right) - \nu \left(\frac{\sigma_3}{E}\right)$$

If strains (σ_2/E) and (σ_3/E) are compressive, the maximum strain in the body is greater than (σ_1/E) . Thus, structural failure can occur below the allowable stress shown in Figure 19. This reduces the factor of safety when it is applied to the allowable stress. If the factor of safety is applied to strain, the allowable strain is

$$\epsilon = \frac{\sigma}{(F.S.)(E)}$$

The foregoing method was applied to a particular example. The results are presented in the following section.

RESULTS

The methods developed in this report were applied to a window 0.42 inches thick. The window was subjected to airloads and an unsymmetrical temperature gradient. The glass was idealized, and internal element loads were computed by a redundant-force computer program. Computer outputs were interpreted as described in the section entitled Interpretation.

Deflections are a direct program output. Figures 12 and 13 show the contributions of airload and thermal deflections to the total deflections in Figure 14. These figures show that the greatest deflections do not occur at the nodes. This means that the maximum surface stresses were not computed.

Stresses were interpreted by the formulae developed in the section on Design Conditions. Figures 15 and 16 show the contributions of mechanical and thermal stresses to the total stresses in Figure 17. These figures show only the tensile stresses that occur on the surfaces of the glass. Compressive stresses also occur, but they are not shown because they are not critical for design. The maximum surface tensile stress of 1293 psi occurs at the boundary on the inner surface. This point is node 15 in Figure 17. The maximum strain is 0.000127 in./in. and the ultimate allowable strain is 0.000295 in./in. The factor of safety based on strain, is 2.32.

EVALUATION

The computer solutions are evaluated by an analyst as a means of controlling these sophisticated computer solutions rather than being controlled by them. To effect this control, the analyst performs approximate hand calculations. Such calculations are not of comparable accuracy, but they reveal any glaring faults in the results obtained from the computer.

Analyses have been developed for flat plates that were subjected to mechanical and thermal loads. Many of the analyses stem from the basic work of Timoshenko. Przemieniecki (Reference 6) also references Timoshenko. Stress formulae are presented for rectangular plates supported at their edges and subjected to uniform pressure and a nonlinear temperature gradient.

The formula for a simply supported panel under uniform pressure is

$$f_{x,y} = \beta_{x,y} p \left(\frac{b}{d} \right)^2 \frac{z}{d}$$

where $\beta_{x,y}$ are functions of the aspect ratio

Thermal stress formulae are given for the effects of mean, linear, and self-equilibrating temperature gradients. The resulting stresses are additive. For the mean temperature, stresses are

$$f_{x,y} = \frac{K \alpha E T_M}{(1-\nu)}$$

where K depends upon the degree of restraint to thermal expansion. If edge restraints in the plane of the panel are largely avoided, these thermal stresses can be made small. For the linear temperature gradient, panel stress formulae are

$$f_{x,y} = \pm \frac{1}{2} \alpha E (\Delta T)$$

for simply supported edges. Self-equilibrating thermal stresses are given by

$$f_{x,y} = \frac{-\alpha E T^*}{(1-\nu)}$$

For X-20A design conditions, stresses were computed assuming simple edge supports and no restraint in the plane of the panel. Stresses for a range of thicknesses are shown

in Figure 18. At 0.42 inch, the combined stress is 770 psi. This is roughly comparable to the computer solution without restraints to bending and in-plane plate expansion. Figure 18 also shows two optimum thicknesses: minimum stress at 0.6 inch and minimum weight at a thickness determined by the factor of safety.

CONCLUSIONS

This report describes a method of structural analysis which completely portrays the behavior of the X-20 front window. The stresses computed were conservative since seal properties are presently undetermined. In the matrix analysis, metal properties were assumed for the seals.

Window weight is largely a function of glass thickness, and minimum weight is a function of the margin of safety. An accurate minimum weight may be determined by analyzing windows of incrementally reduced thickness. The potential weight reduction is about six pounds. The same procedure applies to the minimum strain design which was found by approximate methods.

RECOMMENDATIONS

Based on the structural analysis related herein, the author recommends the following:

- (1) Window seal properties should be established. Doubt in the numerical results is caused by the unknown properties of the seal.
- (2) An optimum glass thickness should be established. Both weight and stress optimums exist. Points favoring an optimum stress are the undesirable brittleness property of glass and vehicle operation in an unexplored environment. Points in favor of an optimum weight are the cost involved in placing weight in orbit and the present material restrictions that limit the allowable re-entry weight.
- (3) There should be an analysis of the window to be tested or a test of the window analyzed. A representative test is the logical conclusion of a design effort.

REFERENCES

1. Design Manual D-5000, Book 89. The Boeing Co., Seattle, Washington. 1961.
2. Argyris, J. H., and Kelsey, S. The Matrix Force Method of Structural Analysis and Some New Applications.
3. Przemieniecki, Dr. J. S. Matrix Structural Analysis. Air Force Institute of Technology, Wright-Patterson Air Force Base, Ohio. 1962.
4. Warren D. D., Castle, R. A., and Gloria, R. C. An Evaluation of the State-Of-The-Art of Thermo-Mechanical Analysis of Structures. WADD TR 61-152. Wright Air Development Division, Wright-Patterson Air Force Base, Ohio. January 1962.
5. Denke, P. H., and Pucket, H. A. Analysis Manual for the Redundant Force Stress Analysis for IBM 709 Computer. Douglas Aircraft Co. Report No. SM-30470. Douglas Aircraft Co. December 1962.
6. Przemieniecki, Dr. J. S. "Design of Transparencies." Journal of the Royal Aeronautical Society. London, England. November 1959.
7. Warren, D. S. A Matrix Method for the Analysis of the Buckling of Structural Panels Subjected to Creep Environments. ASD TDR-62-740. Aeronautical Systems Division, Wright-Patterson Air Force Base, Ohio. November 1962.
8. Timenshenko, S. and Goddier, J. N. Theory of Elasticity. McGraw-Hill Book Company, Inc., New York. 1951. Second Edition.

11

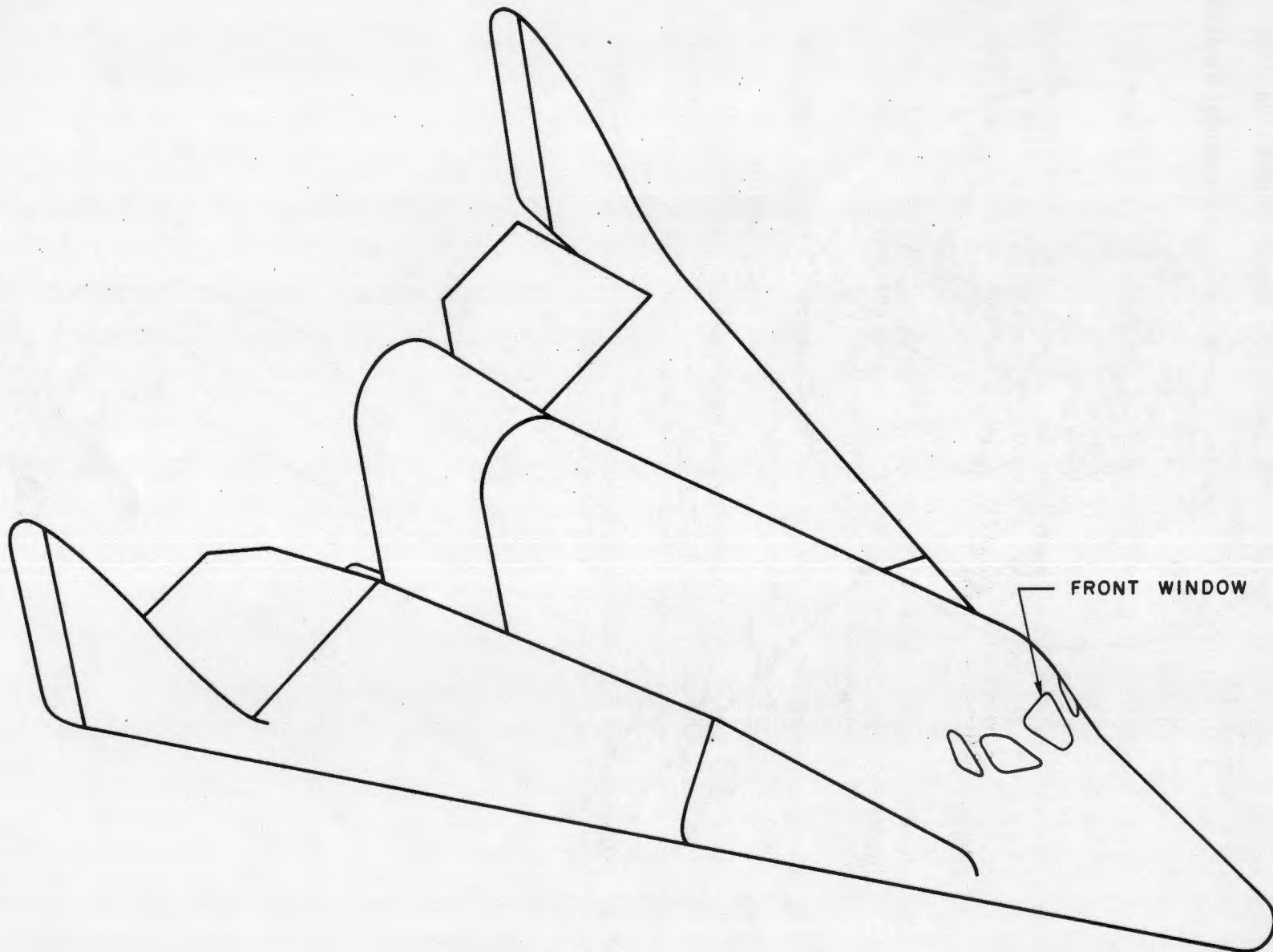


Figure 1. X-20A Glide Re-entry Vehicle

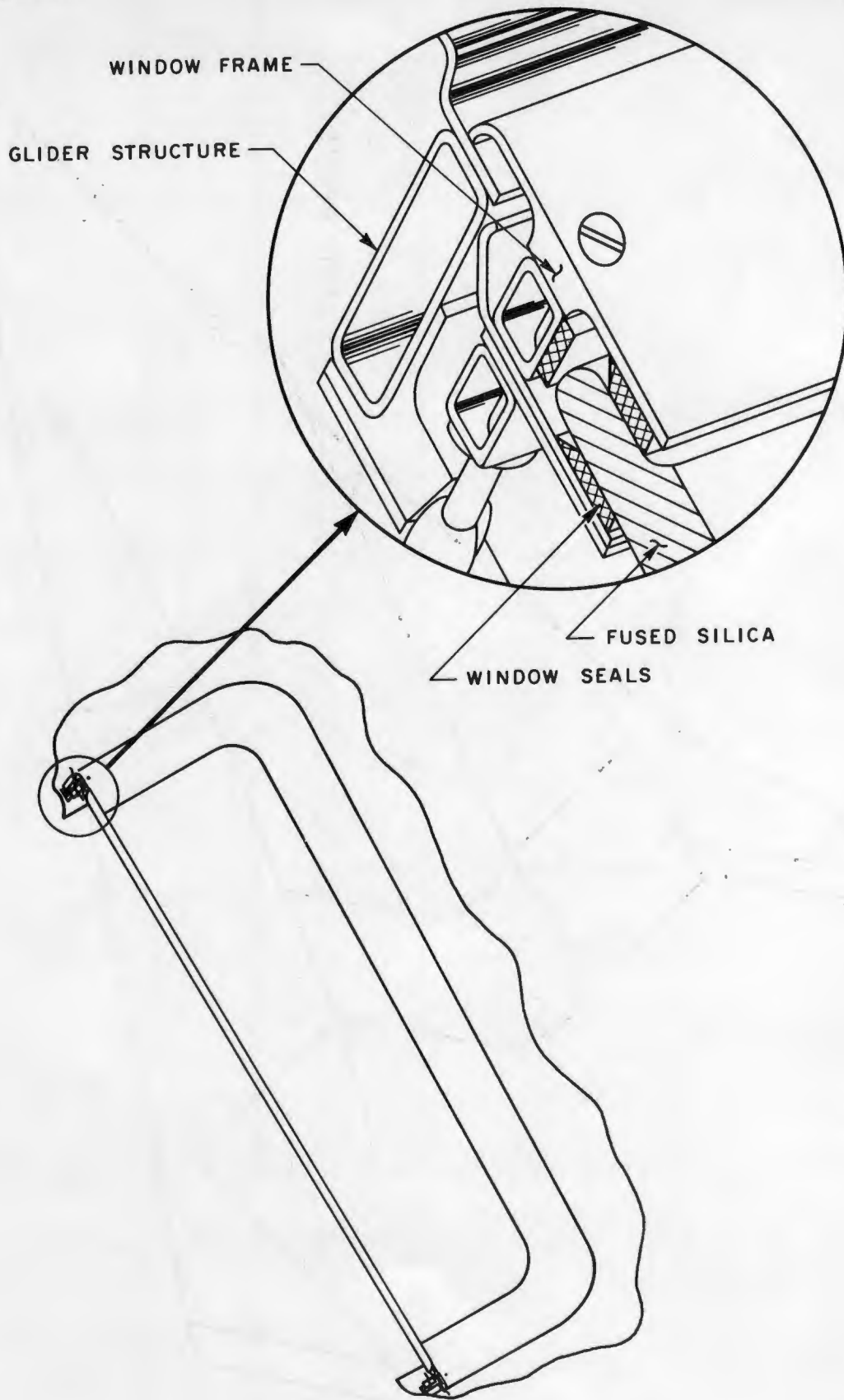


Figure 2. Isometric View of Window

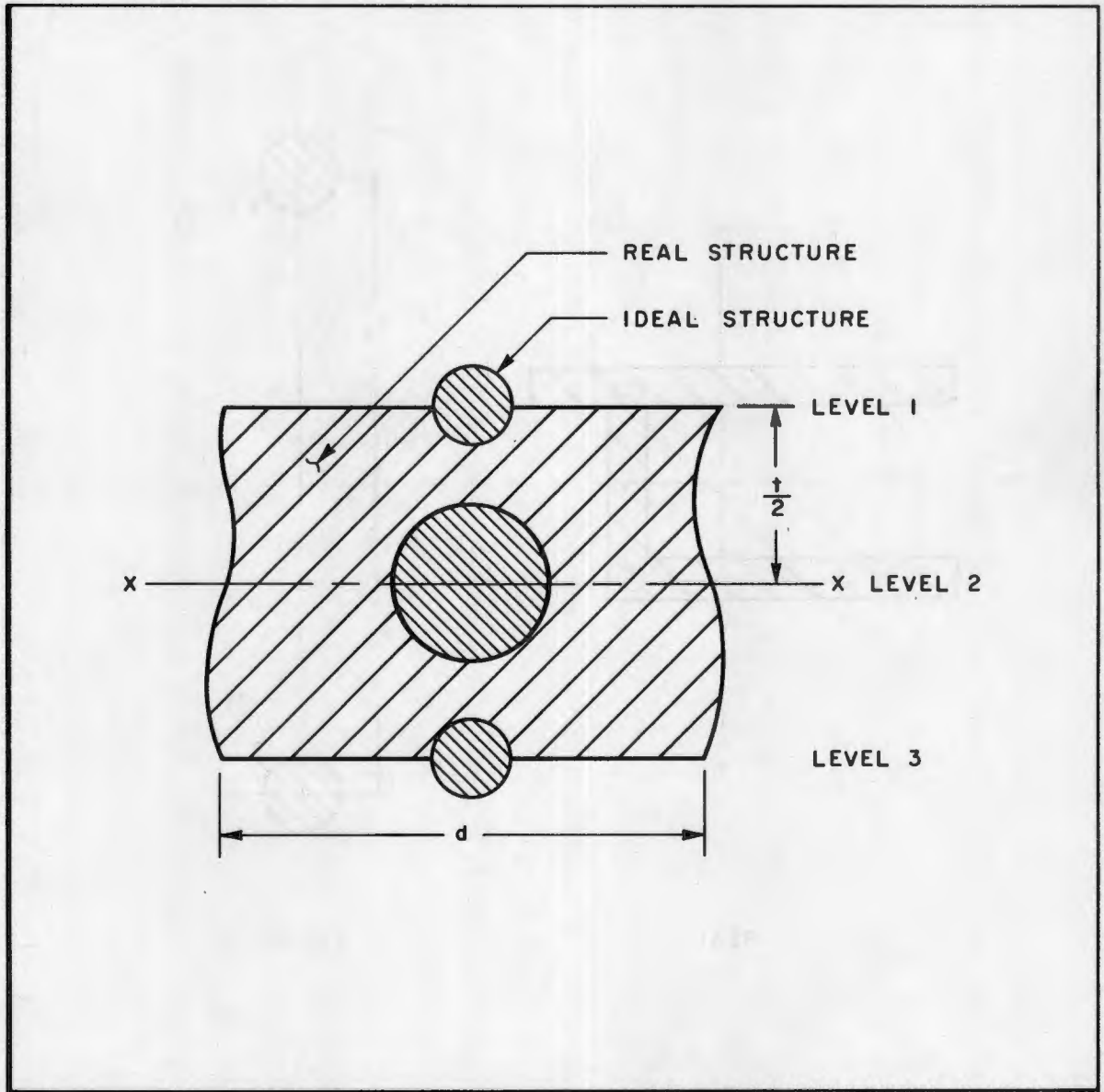


Figure 3. Section of Window Glass

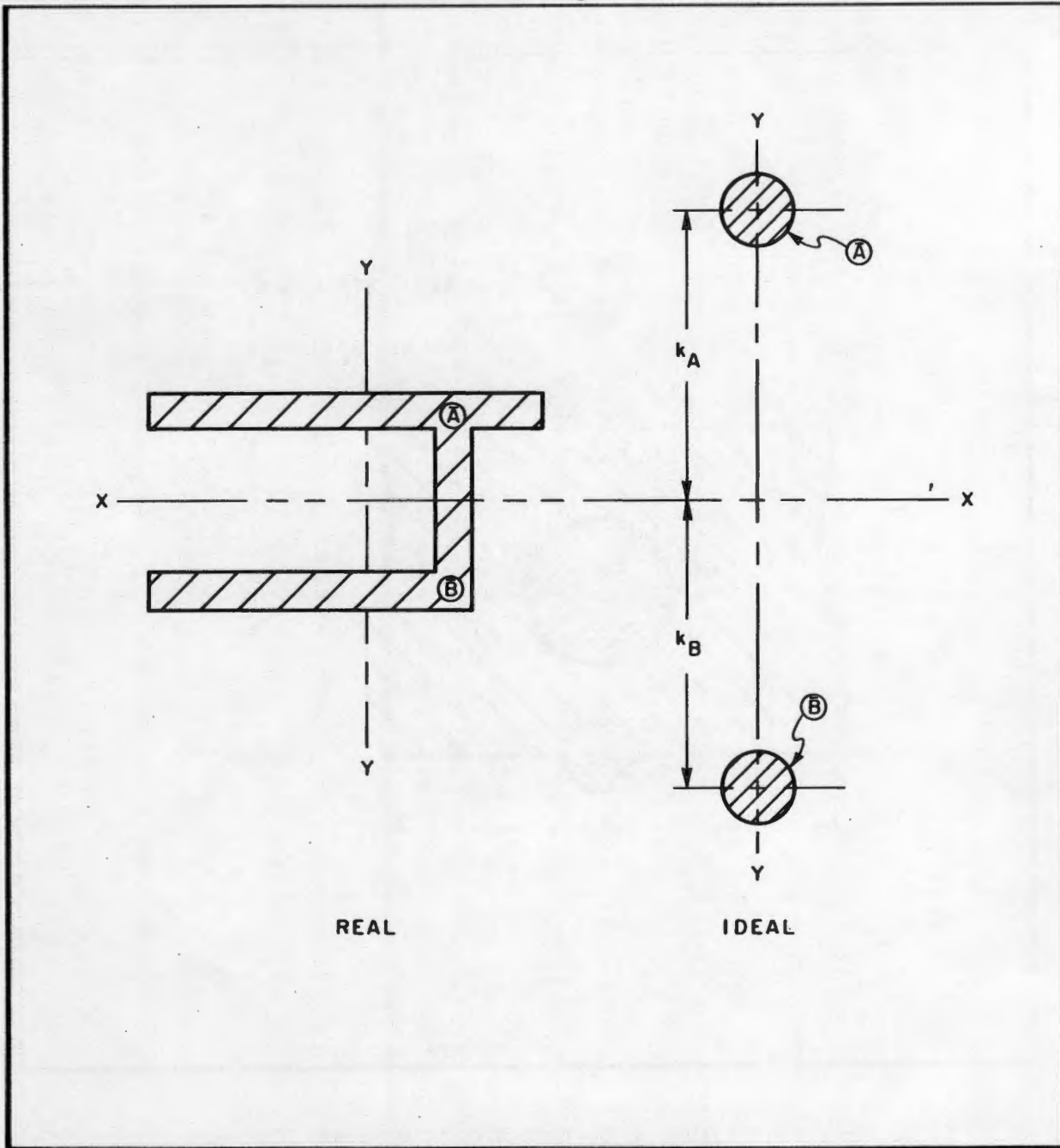


Figure 4. Section of Window Frame

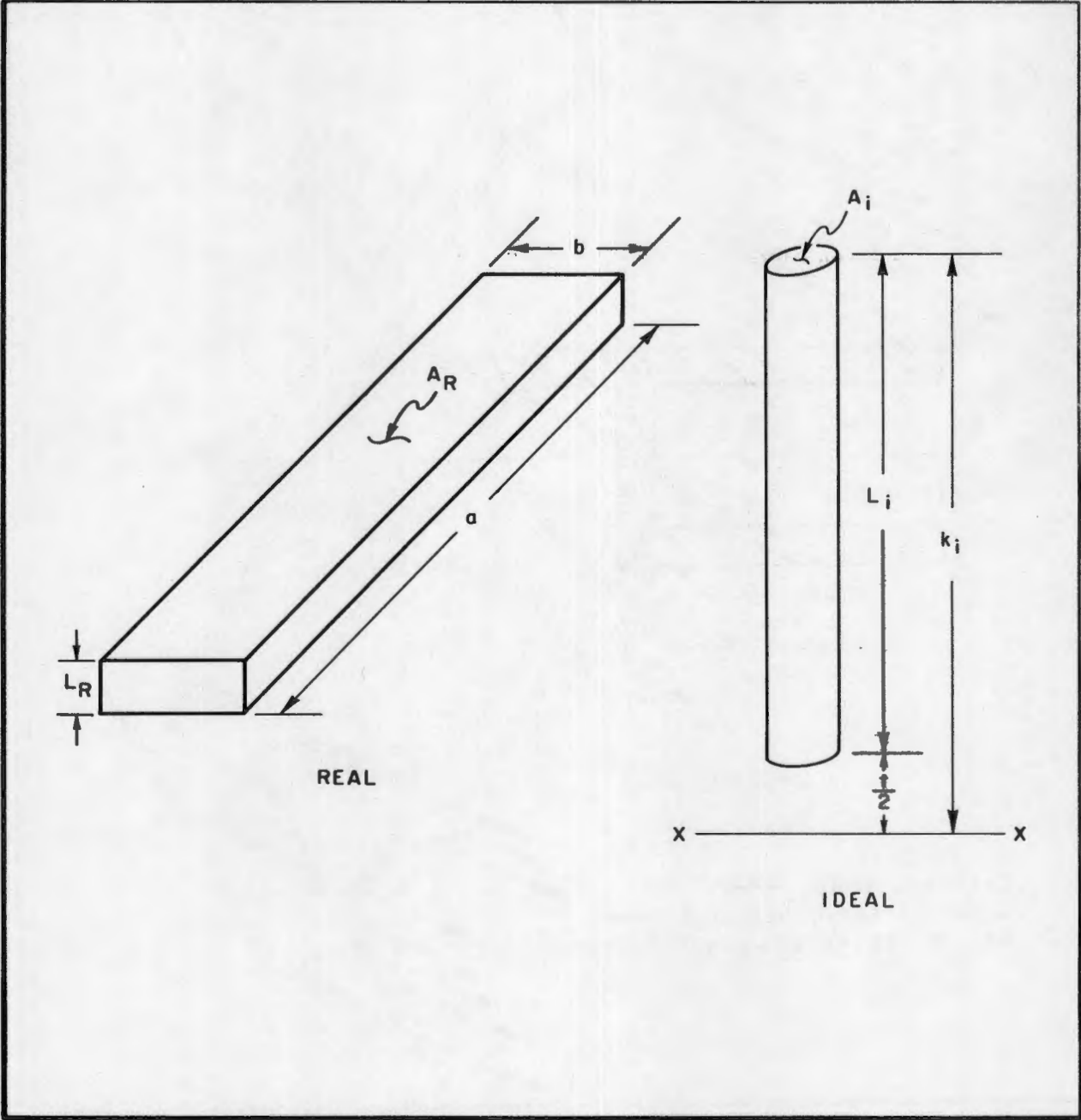


Figure 5. Seal Cross-Section

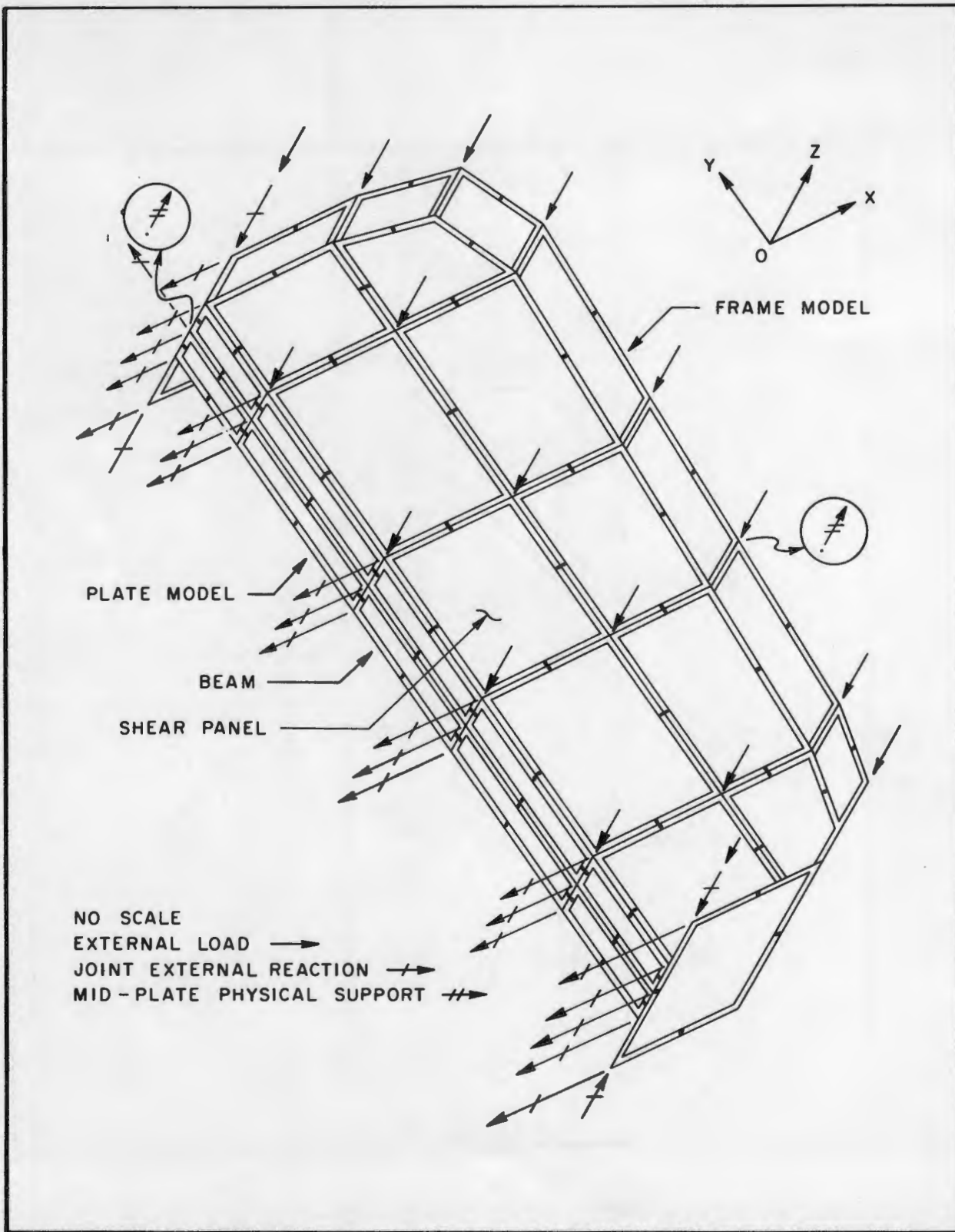


Figure 6. Isometric View of Structural Model

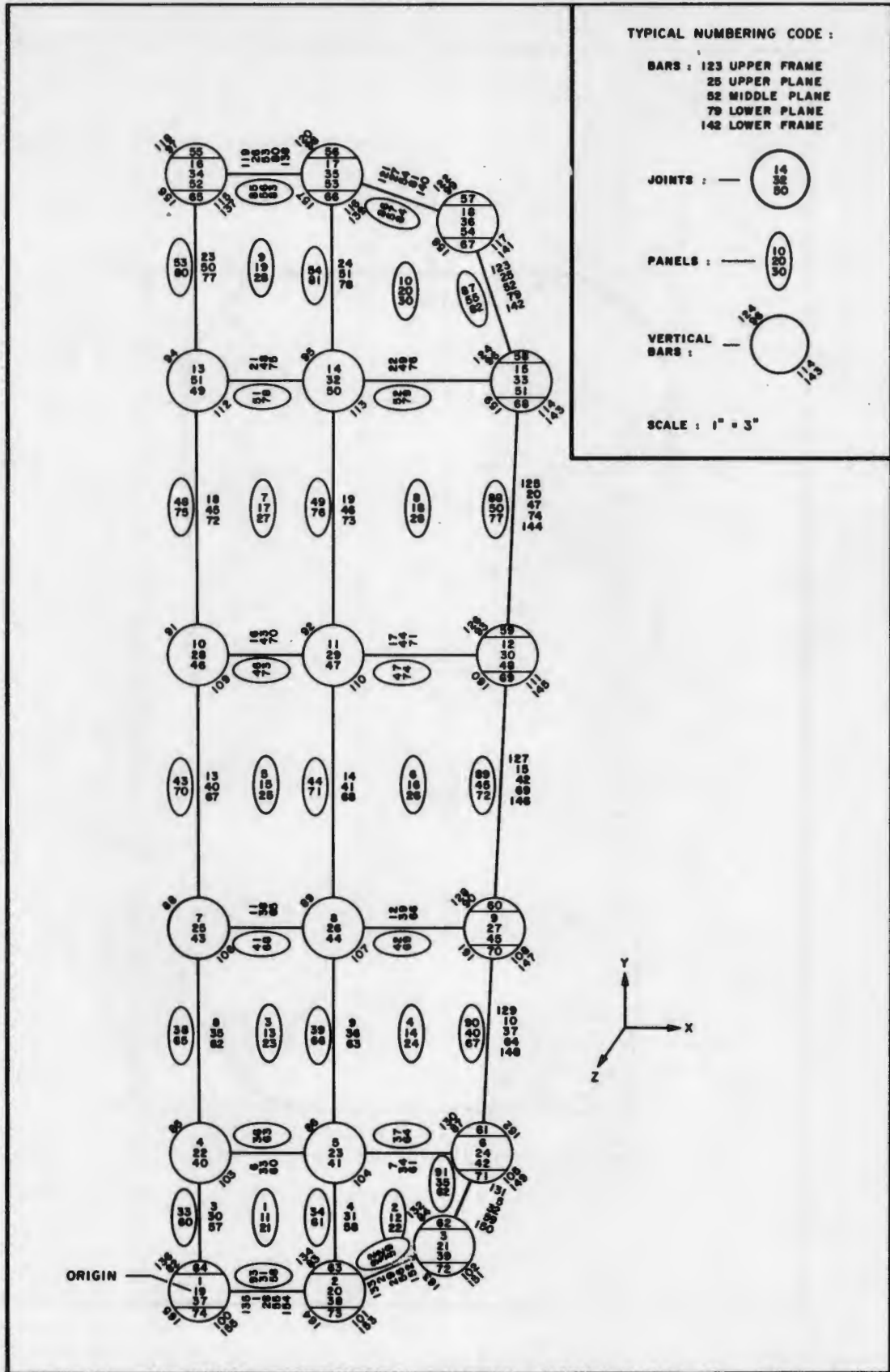


Figure 7. Working Drawing of Structural Model

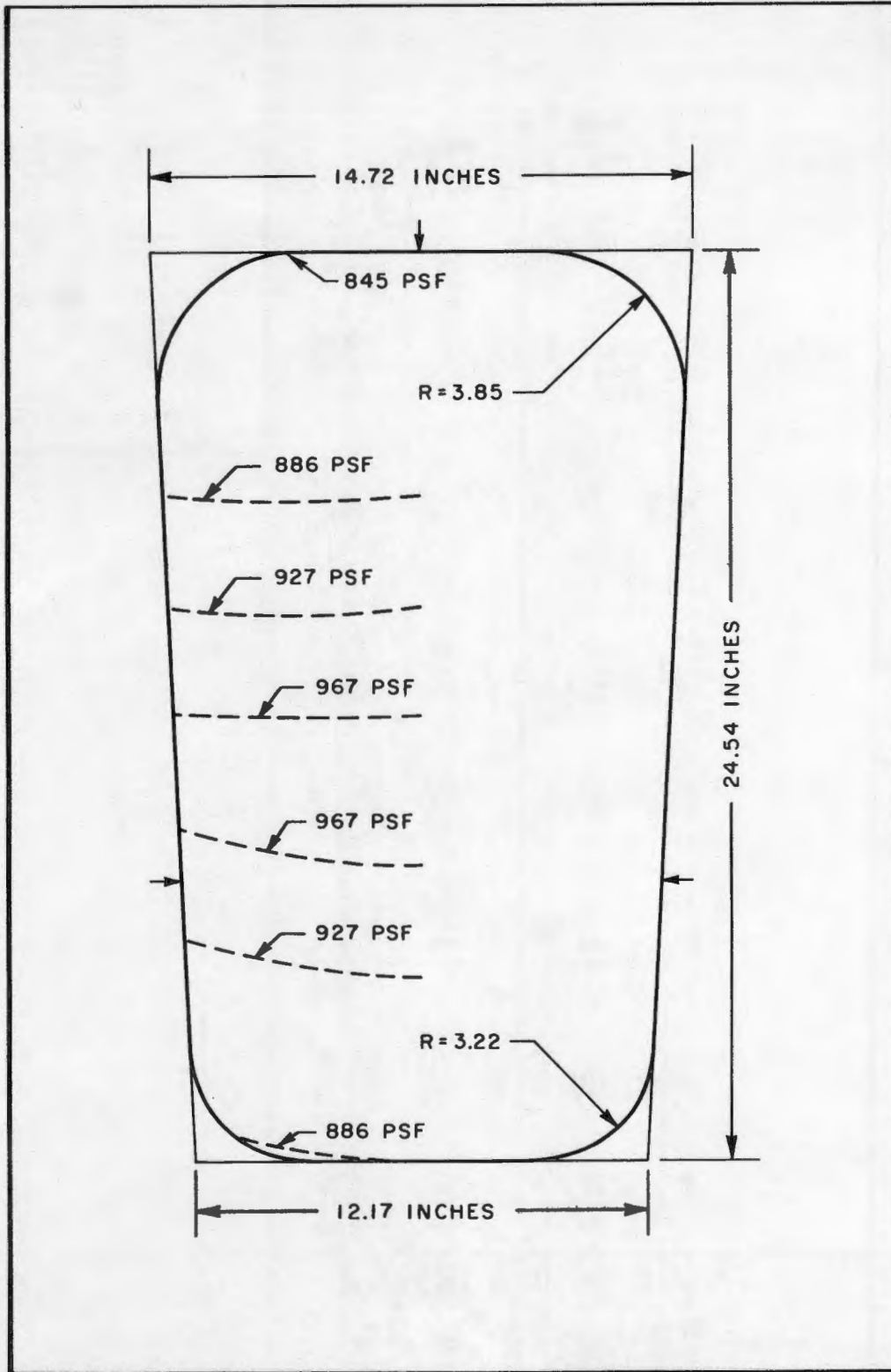


Figure 8. Design Pressure Distribution

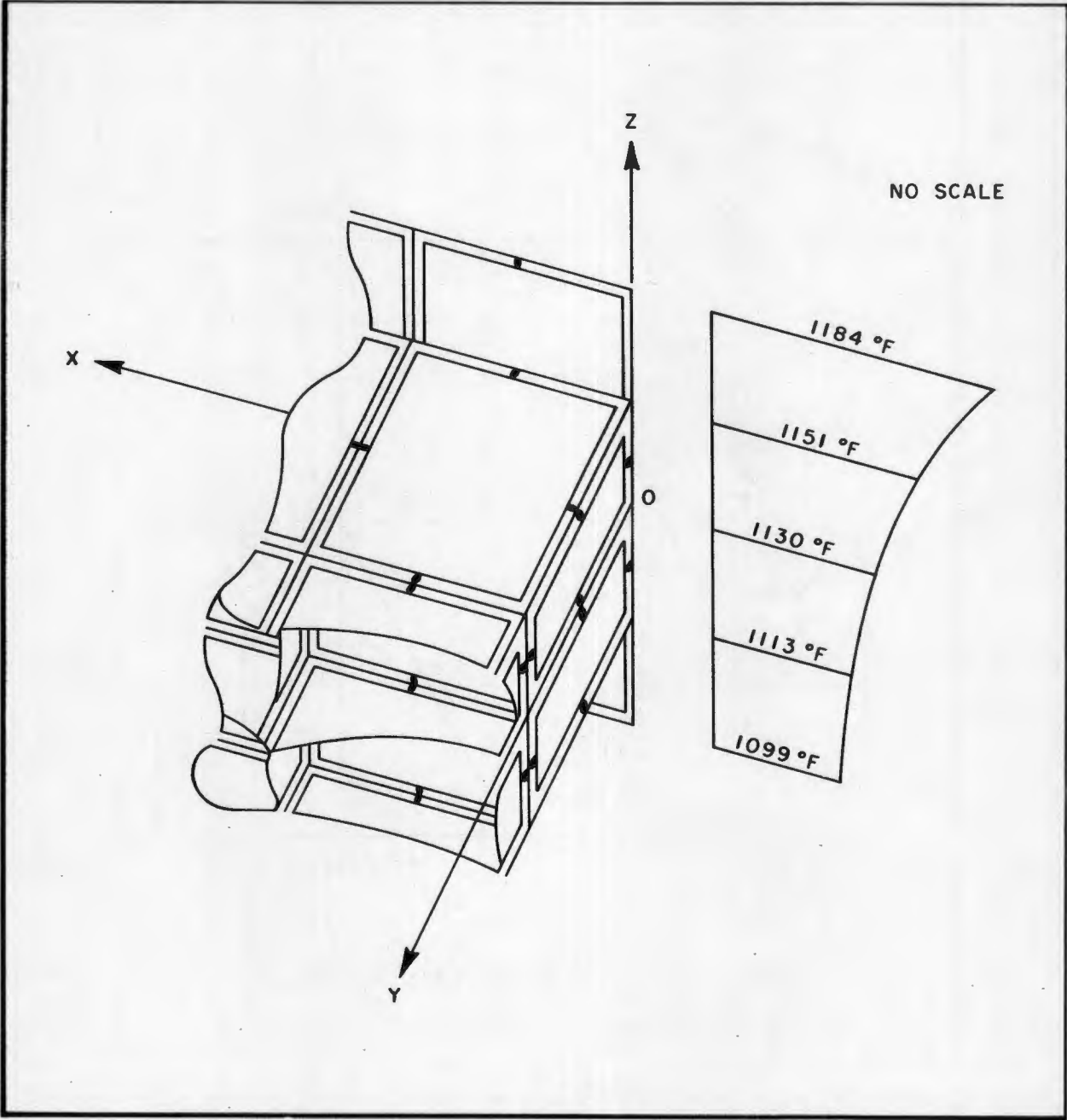


Figure 9. Design Temperature Distribution

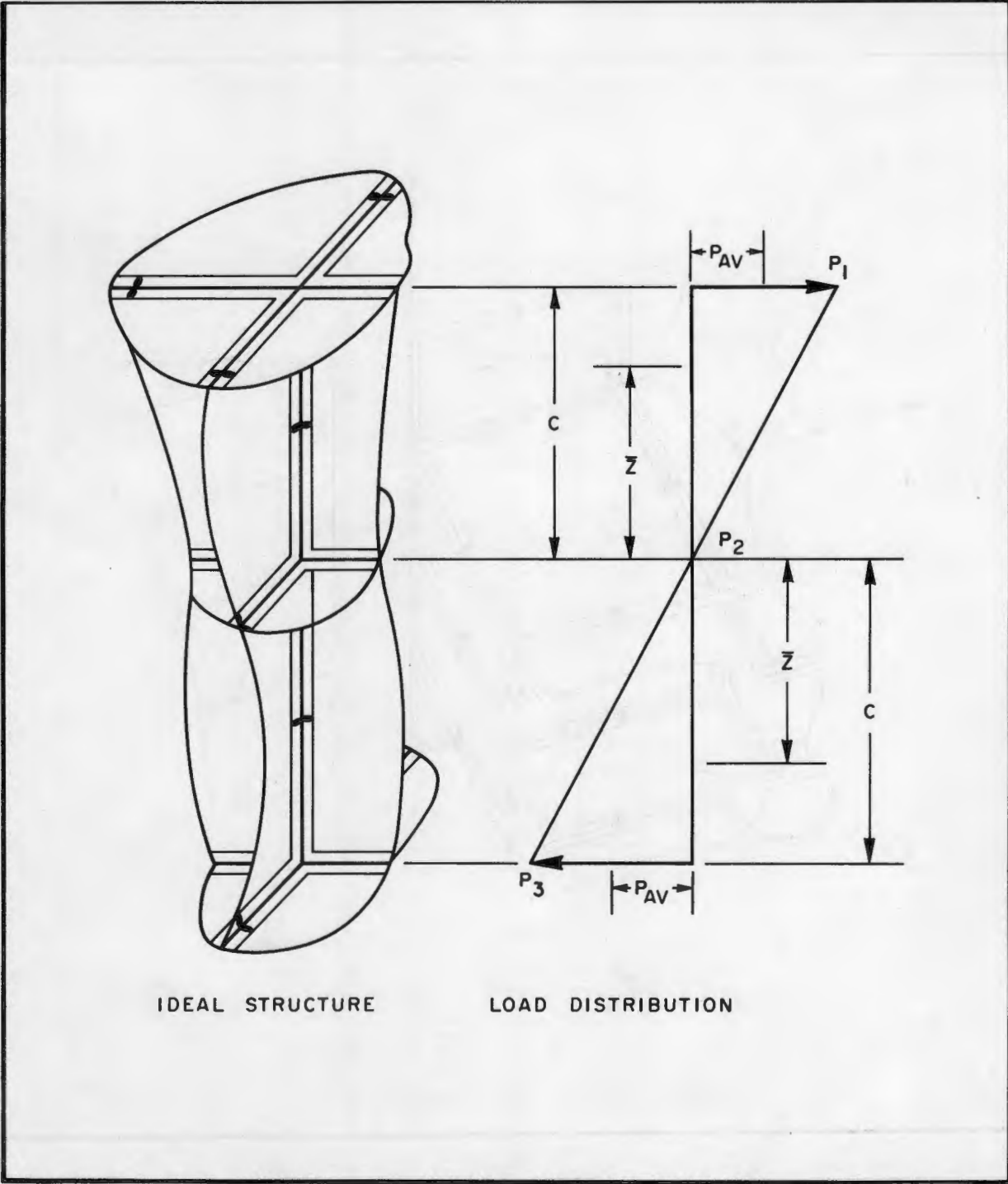


Figure 10. Typical Load Distribution Due to Airloads

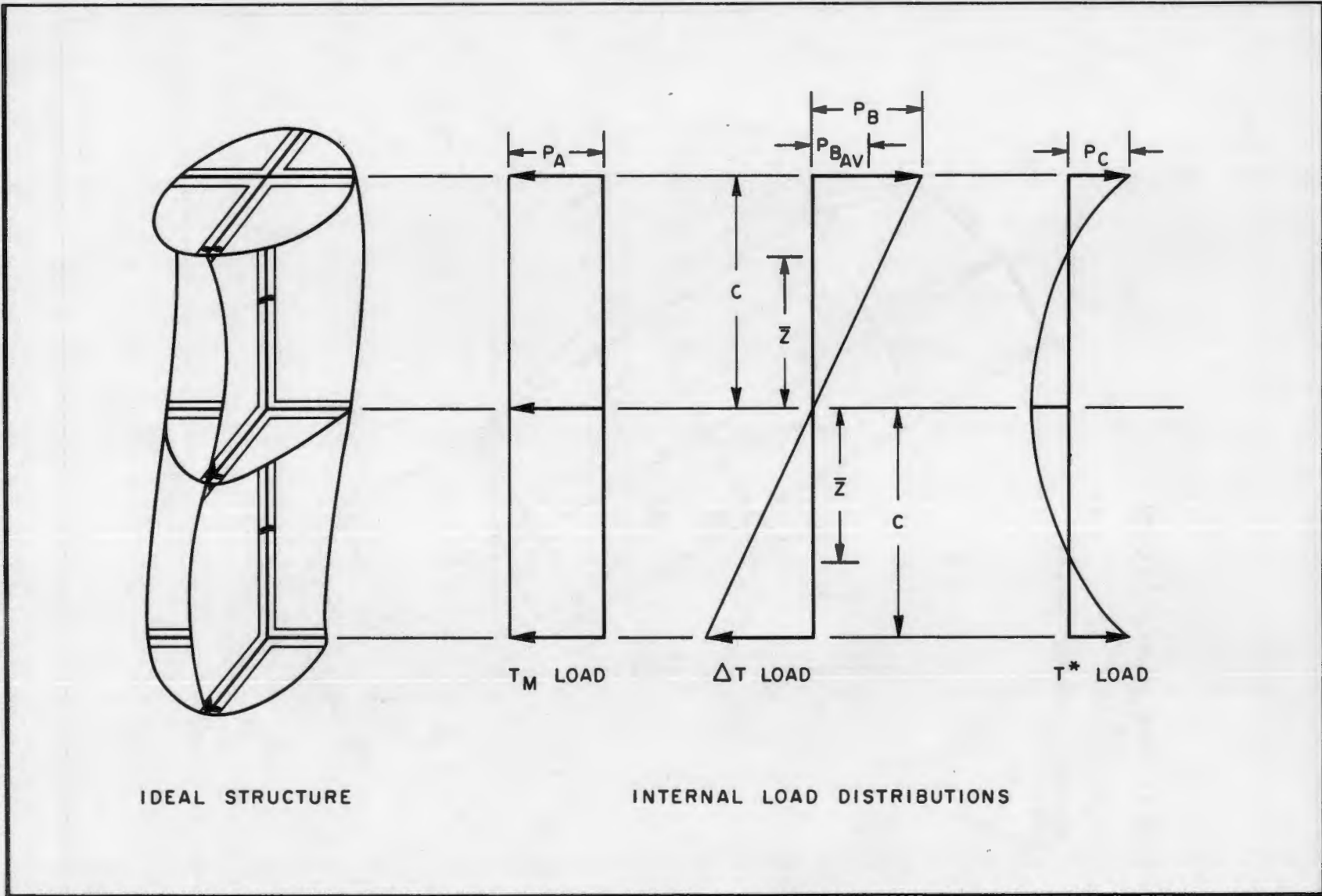


Figure 11. Typical Load Distribution Due to Temperature

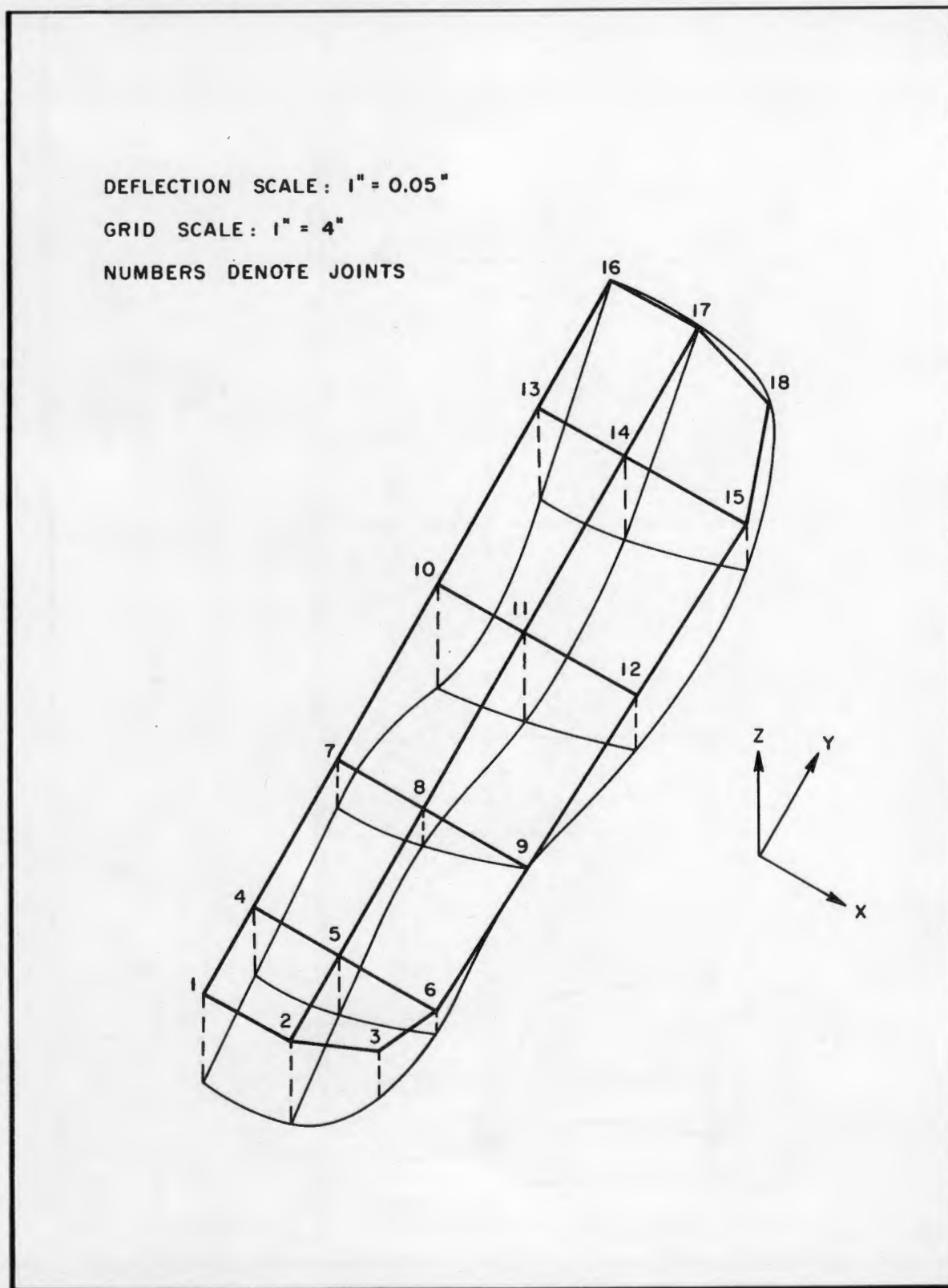


Figure 12. Deflections Due to Airloads

DEFLECTION SCALE : 1" = 0.3"

GRID SCALE : $\frac{1}{4}$ " = 1"

NUMBERS DENOTE JOINTS

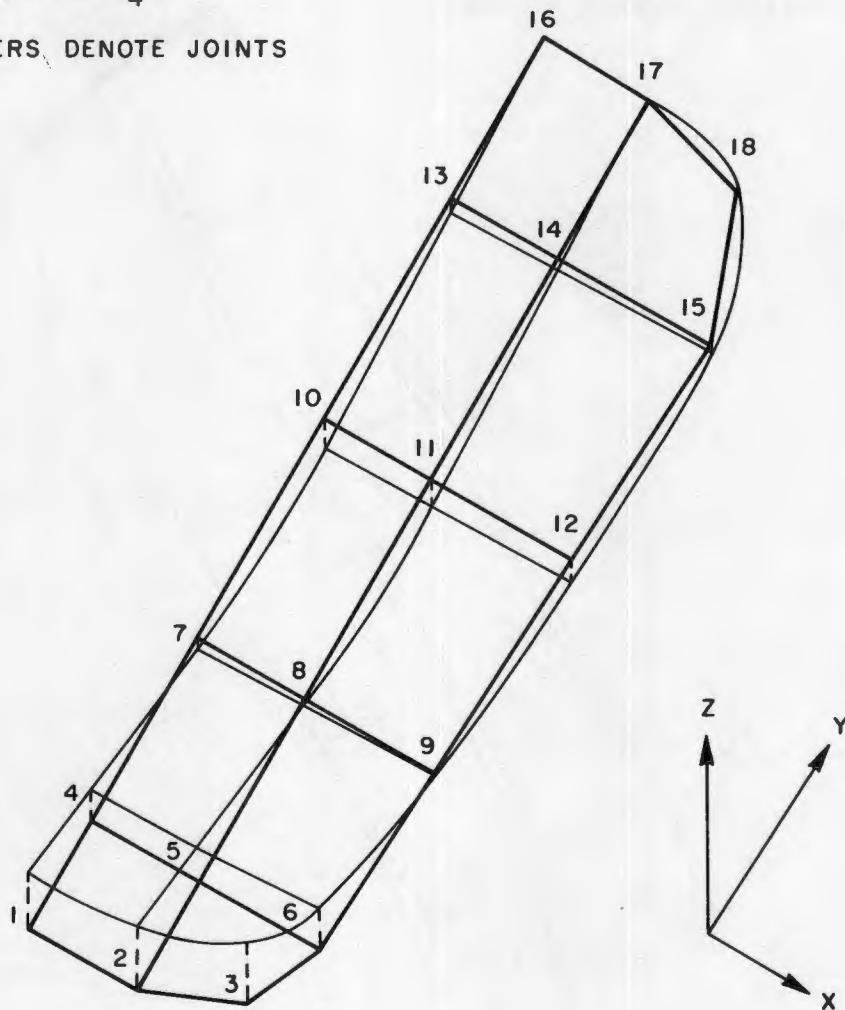


Figure 13. Thermal Deflections

• DEFLECTION SCALE: 1" = 0.01"
GRID SCALE: 1" = 4"
NUMBERS DENOTE JOINTS

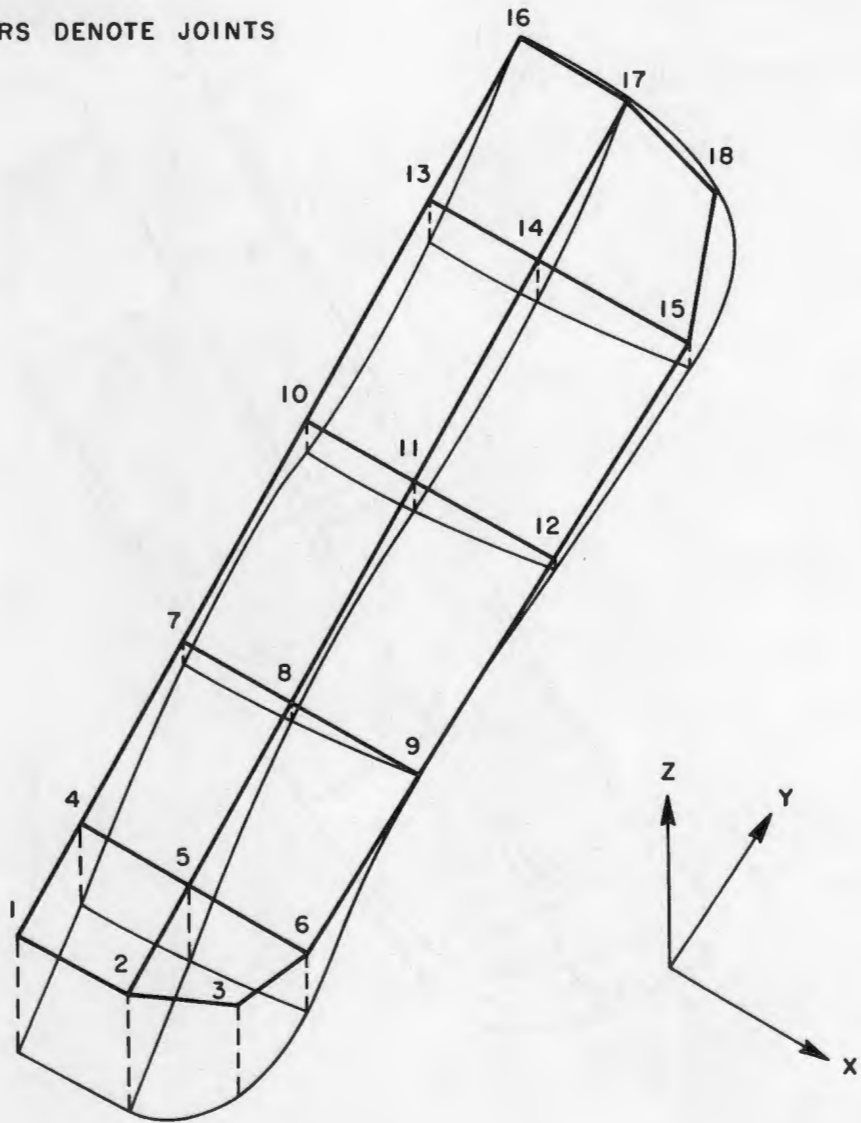


Figure 14. Total Deflections

GRID SCALE : 1" = 4"
STRESS SCALE : 1" = 1000 PSI
NUMBERS DENOTE JOINTS

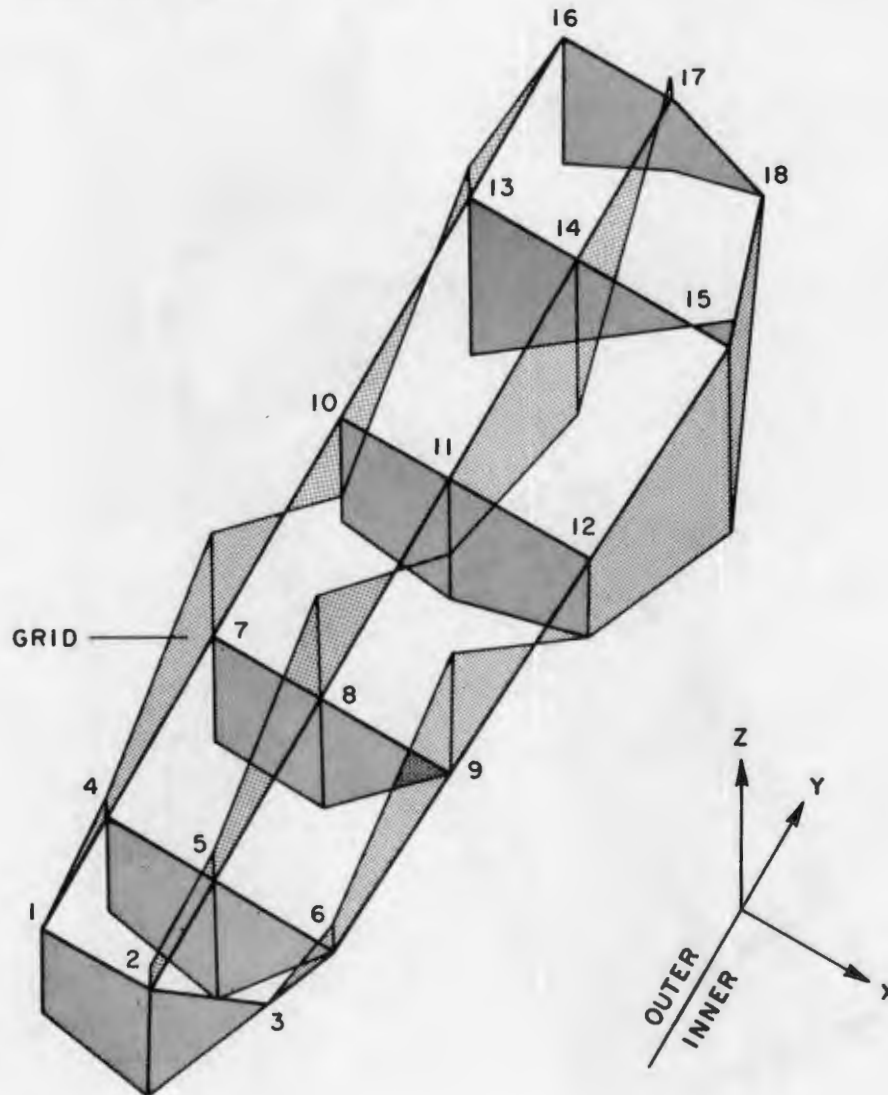


Figure 15. Surface Tensile Stresses Due to Airloads

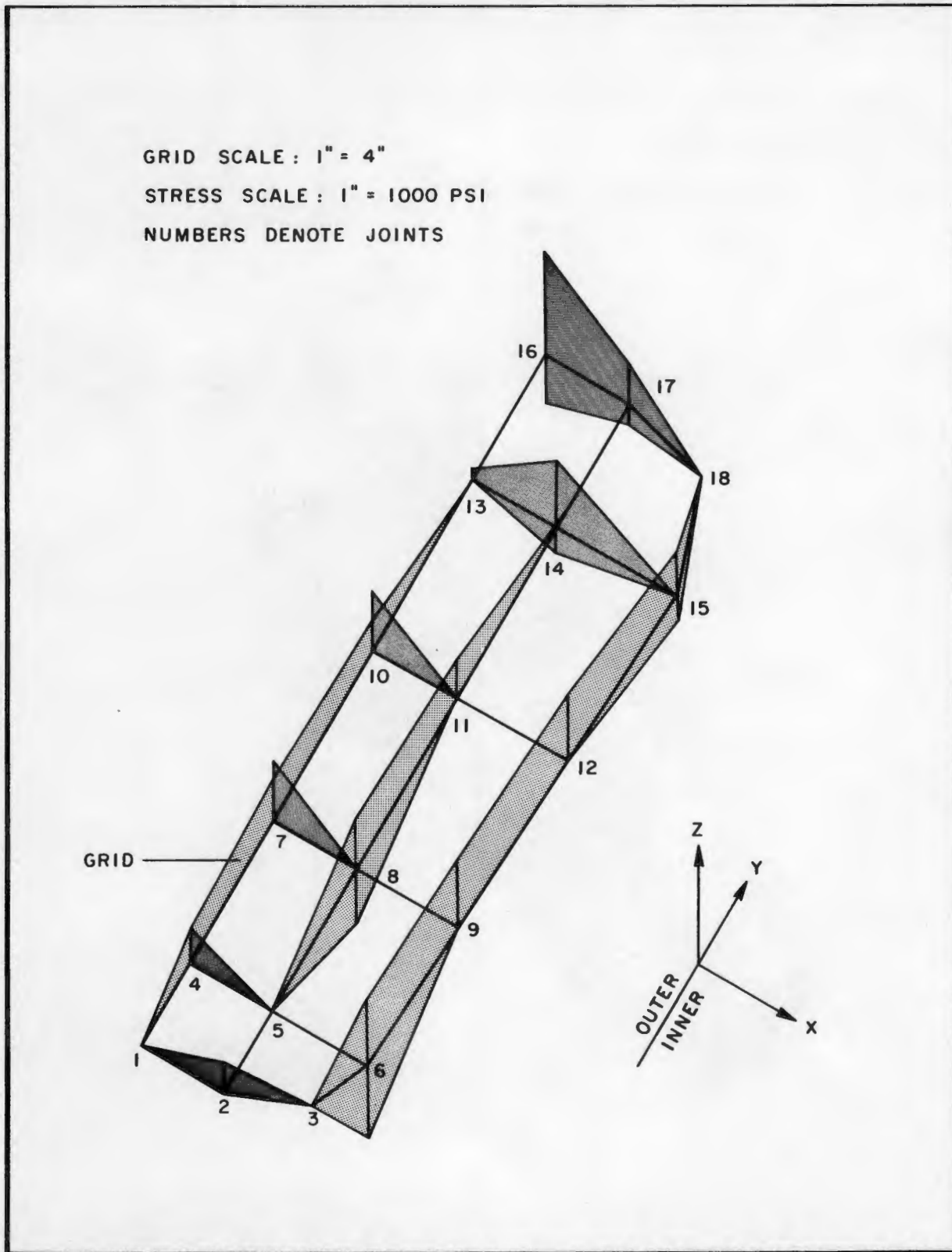


Figure 16. Surface Tensile Stresses Due to Temperature

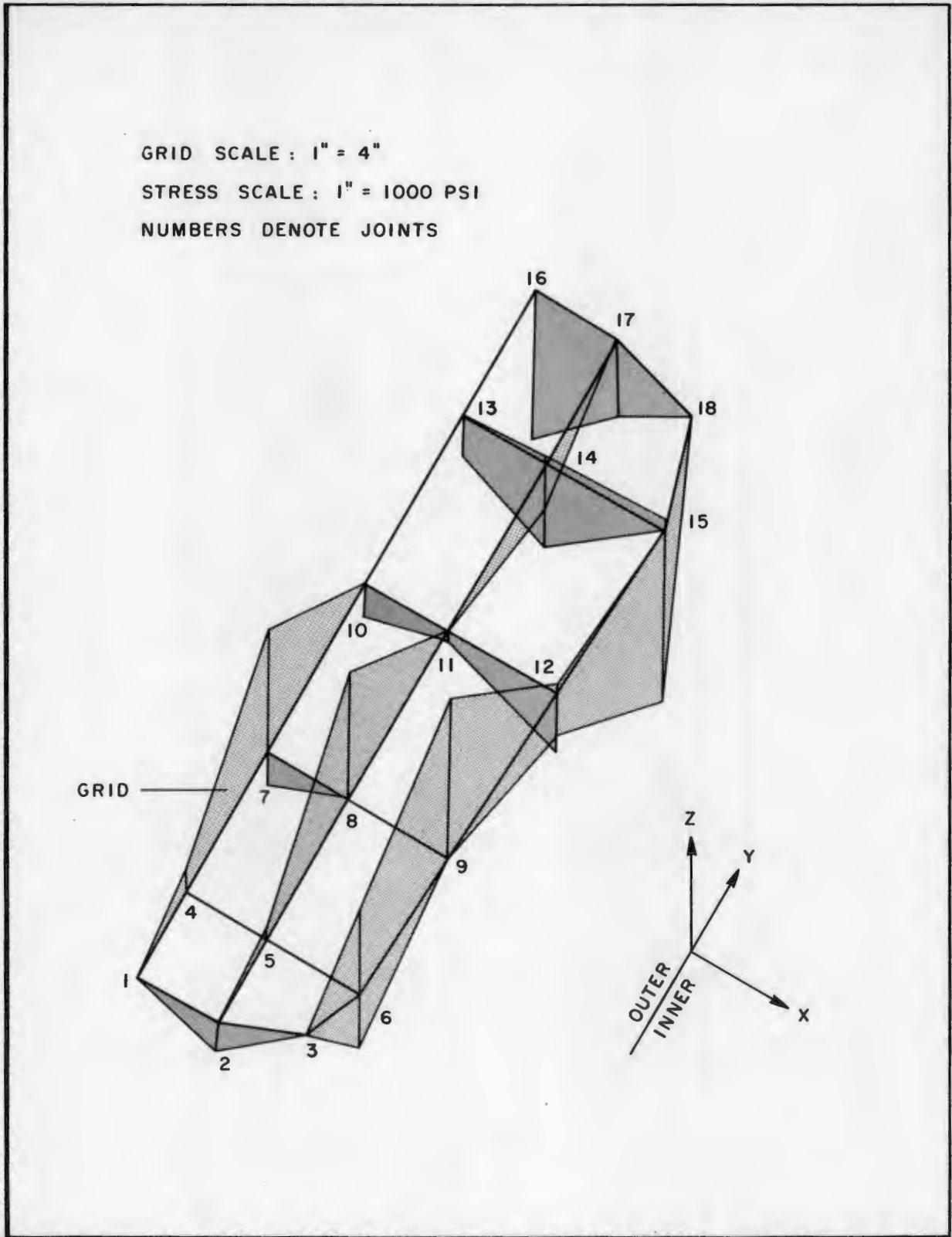


Figure 17. Total Surface Tensile Stresses

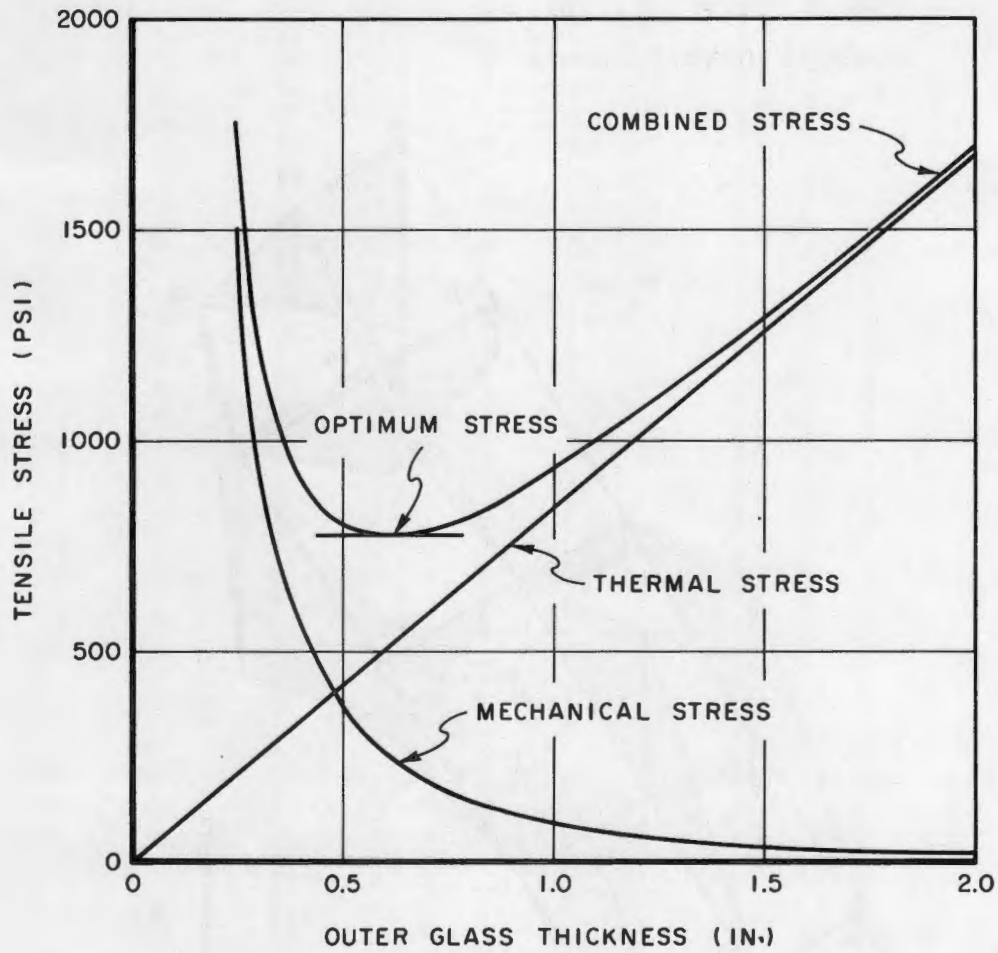


Figure 18. Results of Approximate Stress Analysis

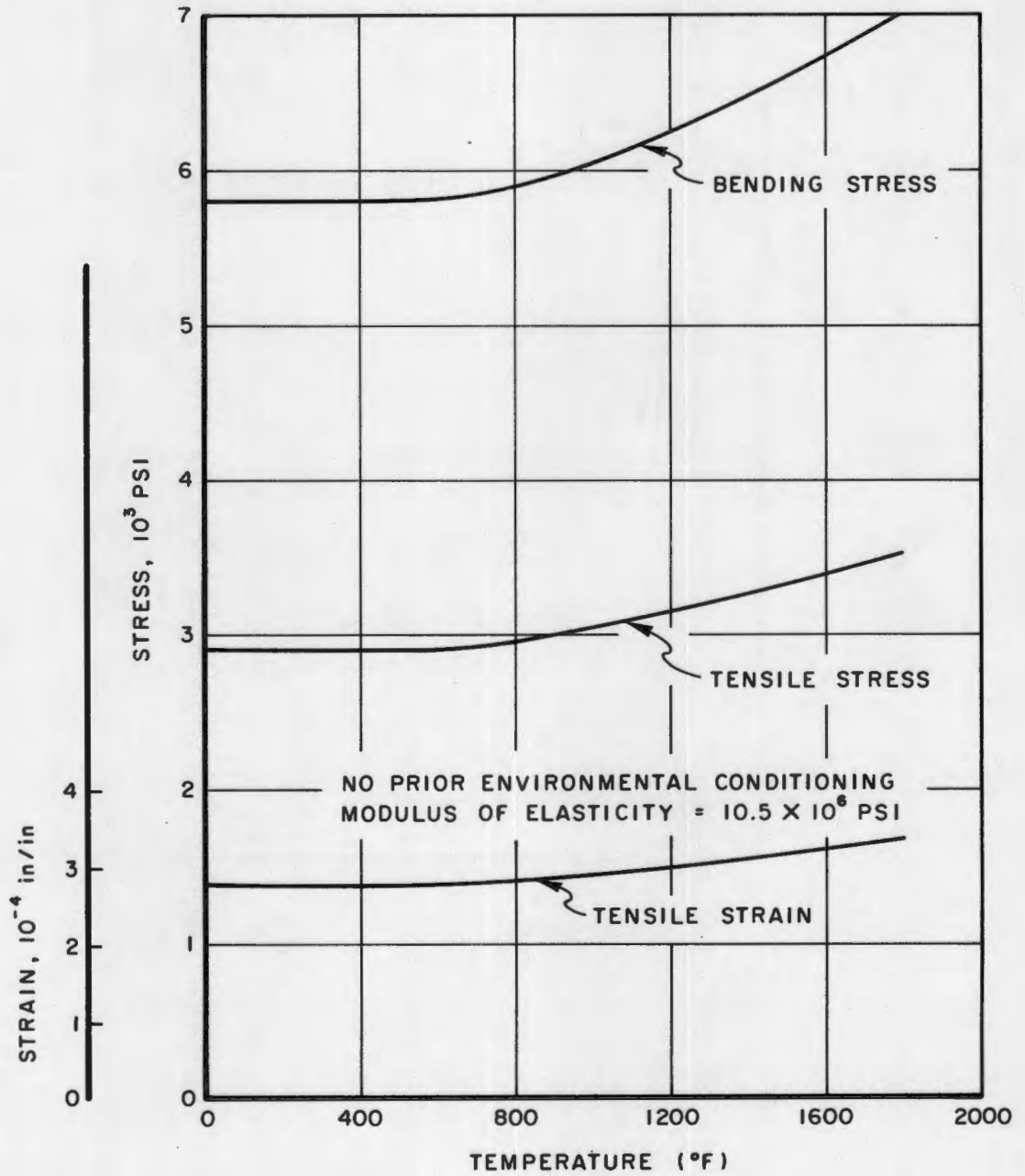


Figure 19. Fused Silica Glass Design Allowables